$W_2Cl_4(NR_2)_2(PR'_3)_2$ Molecules. 4. A New Synthetic Route to Products with a Staggered Conformation. Preparations and Characterizations of $W_2Cl_4(NR_2)_2(PR'_3)_2$ (R = Et, Bu, Hex; R'_3 = Me_3, Et_2H) and an Intermediate Complex $W_2Cl_4(NEt_2)_2(NHEt_2)_2$

F. Albert Cotton,*,† Evgeny V. Dikarev,† N. Nawar,‡ and Wai-Yeung Wong†

Department of Chemistry and Laboratory for Molecular Structure and Bonding, Texas A&M University, College Station, Texas 77843-3255, and Chemistry Department, Faculty of Science, Mansoura University, Mansoura 35516, Egypt

Received August 30, 1996[⊗]

A new and convenient synthetic route to a series of W≡W compounds with the general formula $W_2Cl_4(NR_2)_2(PR'_3)_2$ has been developed. The method has been used in the preparation of $W_2Cl_4(NR_2)_2(PMe_3)_2$ (R = Et (**2**), Bu (**3**), Hex (**4**)) and $W_2Cl_4(NR_2)_2(PEt_2H)_2$ (R = Et (**5**), Bu (**6**), Hex (**7**)). Treatment of $W_2Cl_6(THF)_4$ with the appropriate dialkylamine NHR_2 (R = Et, Bu, Hex) affords an intermediate species having the stoichiometry $W_2Cl_4(NR_2)_2(NHR_2)_2$. This has been verified by single-crystal X-ray diffraction studies for $W_2Cl_4(NEt_2)_2(NHEt_2)_2$ (**1**) with the following crystallographic parameters: orthorhombic space group *Iba*2, a = 11.6704(9) Å, b = 13.336(1) Å, c = 17.321(2) Å, Z = 4. The structure of **1** reveals that the molecule itself deviates from an eclipsed conformation with retention of a strong intramolecular N−H···Cl hydrogen bonding and the torsion angle involving the hydrogen bonded N and Cl atoms is 27.0°. Each W atom is coordinated by a cis set of two Cl and two N atoms with a W−W distance of 2.3084(5) Å. There is a 1.6% orientational disorder of the W−W unit. Subsequent addition of the monodentate phosphines (PMe_3 and PEt_2H) to the intermediate complexes produces a variety of new W_2^{6+} complexes $W_2Cl_4(NR_2)_2(PR'_3)_2$, **2**−**7**, in reasonable yields, depending on the choices of the amines and phosphines. The characterization of **2**−**7** has been accomplished using IR and ^1H and $^{31}P\{^1H\}$ NMR spectroscopy and mass spectrometry. The crystal structures of **2**, **3**, **6**, and **7** are fully described. Crystal data for these compounds are as follows: for **2**, triclinic space group $P\bar{1}$, a = 9.568(2) Å, b = 17.294(7) Å, c = 17.418(5) Å, α = 111.82(3)°, β = 103.11(2)°, γ = 90.72(3)°, Z = 4; for **3**, $P\bar{1}$, a = 12.162(6) Å, b = 14.955(4) Å, c = 18.82 (1) Å, α = 95.66(3)°, β = 97.99(4)°, γ = 91.26(3)°, Z = 4; for **6**, monoclinic space group $P2_1/n$, a = 17.970(3) Å, b = 10.993(2) Å, c = 20.689(4) Å, β = 115.43(1)°, Z = 4; for **7**, $P2_1/c$, a = 15.3937(7) Å, b = 11.473(2) Å, c = 24.977(3) Å, β = 92.33(1)°, Z = 4. The molecular structures of all these phosphine-containing complexes possess a common metal core unit and each entails an essentially staggered $W_2Cl_4N_2P_2$ conformation with the W atoms united by a triple bond (average W−W distance, 2.322 Å). Each molecule adopts a cis configuration with the P and N atoms mutually cis on each W atom, consistent with the stereochemistry of the intermediate species $W_2Cl_4(NR_2)_2(NHR_2)_2$ formed in the first step.

Introduction

Staggered conformations in molecules with metal-metal triple bonds have been observed in numerous molecules of the type $X_3M{\equiv}MX_3$ and $M_2X_nY_{6-n}$, where M represents Mo or W and X and Y represent a variety of univalent groups such as alkyl, halide, NR_2, OR, etc.[1] Later on, more examples of triply-bonded M_2^{6+} complexes (M = Mo or W) in which the metal atoms are four-coordinate became known.[2] Among these, an approach to an $X_4M{\equiv}MX_4$ (M = W) compound was reported by Bradley *et al*., which begins with an edge-sharing bioctahedral species (eqs 1 and 2).[3] The products have strictly eclipsed structures

$$W_2Cl_6(THF)_4 + 6Me_3CNH_2 \rightarrow W_2Cl_4(NHCMe_3)_2(NH_2CMe_3)_2 + 2[Me_3CNH_3]Cl + 4\ THF \quad (1)$$

$$W_2Cl_4(NHCMe_3)_2(NH_2CMe_3)_2 + 2PMe_3 \rightarrow W_2Cl_4(NHCMe_3)_2(PMe_3)_2 + 2Me_3CNH_2 \quad (2)$$

attributable to the presence of N−H···Cl hydrogen bonds even when there is no δ bond between the W atoms. It was our conviction that it should be possible to prepare a broad class of molecules of general formula $W_2Cl_4(NR_2)_2(PR'_3)_2$ (R, R′ = alkyl groups) in a staggered conformation by replacing the amido proton in $W_2Cl_4(NHCMe_3)_2(PR_3)_2$ molecules with an alkyl group, since hydrogen bonds should no longer exist in that case.

In fact, relatively few data are available for W_2^{6+} species having the formula $W_2Cl_x(NR_2)_{6-x}(PR'_3)_2$. To our knowledge, only two complexes of that type have been structurally characterized, viz. $W_2Cl_3(NMe_2)_3(PMe_2Ph)_2$ and $W_2Cl_4(NMe_2)_2$-

† Texas A&M University.
‡ Mansoura University.
⊗ Abstract published in *Advance ACS Abstracts,* January 1, 1997.

(1) (a) Akiyama, M.; Chisholm, M. H.; Cotton, F. A.; Extine, M.; Murillo, C. A. *Inorg. Chem.* **1977**, *16*, 2407 and references therein. (b) Chisholm, M. H.; Cotton, F. A.; Extine, M.; Millar, M.; Stults, B. R. *J. Am. Chem. Soc.* **1976**, *98*, 4486. (c) Cotton, F. A.; Walton, R. A. *Multiple Bonds between Metal Atoms*, 2nd ed.; Oxford University Press: New York, 1993; see also references therein.

(2) (a) Chisholm, M. H. *Polyhedron* **1983**, *2*, 681. (b) Chetcuti, M. J.; Chisholm, M. H.; Huffman, J. C.; Leonelli, J. *J. Am. Chem. Soc.* **1983**, *105*, 292. (c) Chisholm, M. H.; Folting, K.; Hoffman, J. C.; Ratermann, A. L. *Inorg. Chem.* **1984**, *23*, 613. (d) Chisholm, M. H.; Cotton, F. A.; Extine, M. W.; Reichert, W. W. *J. Am. Chem. Soc.* **1978**, *100*, 1727. (e) Chisholm, M. H.; Huffman, J. C.; Kirkpatrick, C. C. *Inorg. Chem.* **1983**, *22*, 1704. (f) Coffindaffer, T. W.; Rothwell, I. P.; Huffman, J. C. *Inorg. Chem.* **1984**, *23*, 1433.

(3) (a) Bradley, D. C.; Errington, R. J.; Hursthouse, M. B.; Short, R. L. *J. Chem. Soc., Dalton Trans.* **1986**, 1305. (b) Bradley, D. C.; Hursthouse, M. B.; Powell, H. R. *J. Chem. Soc., Dalton Trans.* **1989**, 1537.

S0020-1669(96)01069-5 CCC: $14.00

$(PMe_2Ph)_2$.[4] They were formed by phosphine-induced ligand redistribution reactions on $W_2Cl_2(NMe_2)_4$ molecules (eqs 3−5)

$$3W_2Cl_2(NMe_2)_4 + 4L \xrightarrow[\text{toluene}]{25\ ^\circ C} 2W_2Cl_3(NMe_2)_3L_2 + W_2(NMe_2)_6 \quad (3)$$

$$L = PMe_3,\ PMe_2Ph$$

$$2W_2Cl_2(NMe_2)_4 + 2L \xrightarrow[\text{toluene}]{50\ ^\circ C} W_2Cl_4(NMe_2)_2L_2 + W_2(NMe_2)_6 \quad (4)$$

$$L = PMe_2Ph$$

$$4W_2Cl_3(NMe_2)_3L_2 \xrightarrow[\text{toluene}]{60\ ^\circ C} 3W_2Cl_4(NMe_2)_2L_2 + W_2(NMe_2)_6 + 2L \quad (5)$$

$$L = PMe_3,\ PMe_2Ph$$

and both adopt staggered conformations in the solid state. However, a more general synthetic route to this class of compounds is desired so that incorporation of a variety of NR_2 groups rather than only NMe_2 becomes feasible. Herein, we report first the isolation and structural characterization of an intermediate complex $W_2Cl_4(NEt_2)_2(NHEt_2)_2$ formed in the initial step of the reaction of $W_2Cl_6(THF)_4$ with $NHEt_2$ in tetrahydrofuran. From this, a facile synthetic entry that is more convenient and more general for the formation of $W_2Cl_4(NR_2)_2(PR'_3)_2$-type complexes, depending on the choices of R and R′ groups, will then be described. Six new ditungsten(III) complexes $W_2Cl_4(NR_2)_2(PR'_3)_2$ (R = Et, Bu, Hex; R'_3 = Me_3, Et_2H) have been prepared and characterized. The crystal structures of four of them will be presented.

Experimental Section

General Procedures. All manipulations were carried out under a dinitrogen or an argon atmosphere by using standard Schlenk and glovebox techniques. Toluene, hexanes, and THF were distilled under N_2 from potassium/sodium benzophenone ketyl prior to use. PMe_3 and PEt_2H were purchased from Strem Chemicals and used without further purification. WCl_4 was prepared by refluxing WCl_6 and $W(CO)_6$ in chlorobenzene,[5] and stored in glass vials prior to use. All dialkylamines were purchased from Aldrich, Inc., and used as received. A general literature method was used to prepare $W_2Cl_6(THF)_4$ using Na−Hg as the reducing agent.[6]

Syntheses. (i) $W_2Cl_4(NEt_2)_2(NHEt_2)_2$ (1). Diethylamine (0.48 mL, 4.62 mmol) was added by syringe to a stirred solution of $W_2Cl_6(THF)_4$ prepared by reduction of WCl_4 (0.5 g, 1.54 mmol) with 1 equiv of Na−Hg (0.4%) in tetrahydrofuran (15 mL). The color of the solution started to change from greenish-yellow to reddish-brown and the mixture was allowed to stir for 12 h to ensure completion of the reaction. The solution was then filtered through Celite to remove Hg and NaCl. When a mixture of isomeric hexanes was carefully layered on this filtrate, orange crystals of $W_2Cl_4(NEt_2)_2(NHEt_2)_2$ (0.43 g, 70% based on WCl_4) were obtained after one week at −15 °C.

IR data (cm^{-1}): 3182 (s), 1438 (s), 1400 (s), 1356 (s), 1337 (w), 1323 (vw), 1310 (w), 1282 (w), 1262 (vw), 1205 (m), 1182 (m), 1157 (s), 1146 (m), 1118 (w), 1096 (s), 1060 (s), 1044 (s), 1037 (s), 1008 (vs), 920 (w), 899 (w), 876 (s), 842 (m), 793 (s), 776 (vs), 614 (w), 594 (m), 548 (m).

^{1}H NMR data ($CDCl_3$, 24 °C, δ): 1.05−1.46 (m, 24H, all CH_3), 2.49 (m, 4H, amido and amino NCH_2CH_3), 3.01 (m, 8H, amido and amino NCH_2CH_3), 4.82 (m, 2H, amido proximal NCH_2CH_3), 5.26 (m, br, 2H, N−H), 5.97 (m, 2H, amido proximal NCH_2CH_3).

FAB/DIP MS (NBA, *m/z*): 800 ($[M]^+$), 765 ($[M - Cl]^+$), 728 ($[M - 2Cl]^+$ or $[M - NHEt_2]^+$ or $[M - NEt_2]^+$), 690 ($[M - Cl - NHEt_2]^+$ or $[M - Cl - NEt_2]^+$), 654 ($[M - 2Cl - NHEt_2]^+$ or $[M - 2Cl - NEt_2]^+$ or $[M - 2NHEt_2]^+$ or $[M - NHEt_2 - NEt_2]^+$ or $[M - 2NEt_2]^+$).

(ii) $W_2Cl_4(NEt_2)_2(PMe_3)_2$ (2). To the filtrate (15 mL) in part i was added excess PMe_3 (0.16 mL, more than 2 equiv) via syringe, and the color of the solution became dark-red in a few minutes. Stirring was continued for 1 h, after which all the volatile components of the mixture were removed under vacuum. The residual dark-red solid was then redissolved in hot toluene (15 mL) to give a deep red solution. An abundant crop of red crystals of **2** (0.34 g, 55% based on starting WCl_4) formed in 2 days by layering hexanes over the toluene extract at room temperature. Compound **2** was stable in air as a solid, but it was quickly oxidized (or disproportionated) in solutions at room temperature to leave some purple crystalline products. We were able to identify one of them as the mononuclear W(IV) species $WOCl_2(PMe_3)_3$, based on $^{31}P\{^1H\}$ NMR data and unit cell parameters for the crystals.[7]

IR data (cm^{-1}): 1416 (m), 1367 (s), 1356 (m), 1302 (m), 1286 (m), 1281 (s), 1261 (w), 1183 (w), 1144 (m), 1098 (m), 1067 (w), 1040 (m), 1001 (m), 950 (vs), 880 (m), 857 (w), 841 (m), 802 (s), 744 (m), 675 (w).

^{1}H NMR data (benzene-d_6, 24 °C, δ): 0.89 (t, J = 7.0 Hz, 6H, distal CH_3), 1.16 (t, J = 7.0 Hz, 6H, proximal CH_3), 1.52 (d, J = 9.8 Hz, 18H, PMe_3), 2.03 (m, 2H, distal CH_2), 2.21 (m, 2H, distal CH_2), 4.75 (m, 2H, proximal CH_2), 5.97 (m, 2H, proximal CH_2).

$^{31}P\{^1H\}$ NMR data (benzene-d_6, 19 °C, δ): −4.10 (s, $^1J_{W-P}$ = 311 Hz. $^3J_{P-P}$ = 5.1 Hz).

FAB/DIP MS (NBA, *m/z*): 806 ($[M]^+$), 771 ($[M - Cl]^+$), 735 ($[M - 2Cl]^+$ or $[M - NEt_2]^+$), 693 ($[M - Cl - PMe_3]^+$), 659 ($[M - 2Cl - PMe_3]^+$ or $[M - NEt_2 - PMe_3]^+$), 619 ($[M - Cl - 2PMe_3]^+$), 582 ($[M - 2Cl - 2PMe_3]^+$ or $[M - NEt_2 - 2PMe_3]^+$).

(iii) $W_2Cl_4(NBu_2)_2(PMe_3)_2$ (3). Dibutylamine (0.78 mL, 4.62 mmol) was added by syringe to a stirred solution of $W_2Cl_6(THF)_4$ (from 0.5 g WCl_4) in tetrahydrofuran (15 mL). After 12 h, the reddish-brown solution was filtered through Celite, and excess PMe_3 (0.16 mL) was then added via syringe. The reaction mixture was stirred for 1 h, after which the volatile components were removed under reduced pressure and the resulting solid was redissolved in hexanes (20 mL), concentrated, and cooled to −15 °C. Bright red rhomboidal crystals of **3** formed after 2 days, and were collected by filtration, washed with cold hexanes (5 mL), and dried under vacuum. Yield: 0.41 g; 58% based on WCl_4.

IR data (cm^{-1}): 1416 (m), 1368 (m), 1345 (sh), 1302 (m), 1283 (m), 1261 (s), 1170 (w), 1144 (m), 1095 (s, br), 1019 (s, br), 955 (vs), 909(m), 859 (w), 801 (s).

^{1}H NMR data (benzene-d_6, 24 °C, δ): 0.73 (t, J = 7.2 Hz, 6H, distal CH_3), 0.95 (m, 4H, $NCH_2(CH_2)_2CH_3$), 1.06 (t, J = 7.2 Hz, 6H, proximal CH_3), 1.42 (m, 8H, $NCH_2(CH_2)_2CH_3$), 1.60 (d, J = 9.9 Hz, 18H, PMe_3), 1.86 (m, br, 4H, $NCH_2(CH_2)_2CH_3$), 2.13 (m, 2H, distal $NCH_2(CH_2)_2CH_3$), 2.52 (m, 2H, distal $NCH_2(CH_2)_2CH_3$), 4.96 (m, 2H, proximal $NCH_2(CH_2)_2CH_3$), 6.00 (m, 2H, proximal $NCH_2(CH_2)_2CH_3$).

$^{31}P\{^1H\}$ NMR data (benzene-d_6, 19 °C, δ): −4.45 (s, $^1J_{W-P}$ = 313 Hz, $^3J_{P-P}$ = 5.2 Hz).

FAB/DIP MS (NBA, *m/z*): 918 ($[M]^+$), 883 ($[M - Cl]^+$), 842 ($[M - PMe_3]^+$), 805 ($[M - Cl - PMe_3]^+$), 790 ($[M - NBu_2]^+$), 769 ($[M - 2Cl - PMe_3]^+$), 754 ($[M - Cl - NBu_2]^+$), 729 ($[M - Cl - 2PMe_3]^+$), 715 ($[M - NBu_2 - PMe_3]^+$), 677 ($[M - Cl - NBu_2 - PMe_3]^+$), 638 ($[M - NBu_2 - 2PMe_3]^+$).

(iv) $W_2Cl_4(NHex_2)_2(PMe_3)_2$ (4). To a stirred solution of $W_2Cl_6(THF)_4$ (from 0.5 g WCl_4) in tetrahydrofuran (15 mL) was added 1.08 mL of dihexylamine (4.62 mmol) by syringe, producing a red-brown mixture. The solution was stirred for 12 h at room temperature and then filtered through Celite. PMe_3 (0.16 mL) was added subsequently to the filtrate, and the dark reddish-brown slurry was stirred for 1 h, after which the solvent was removed *in vacuo*. The residue was thoroughly dried, then extracted with warm hexanes (15 mL). Red

(4) Ahmed, K. J.; Chisholm, M. H.; Folting, K.; Huffman, J. C. *Inorg. Chem.* **1985**, *24*, 4039.
(5) Schrock, R. R.; Sturgeoff, L. G.; Sharp, P. R. *Inorg. Chem.* **1983**, *22*, 2801.
(6) (a) Chisholm, M. H.; Eichhorn, B. W.; Folting, K.; Huffman, J. C.; Ontiveros, C. D.; Streib, W. E.; Van Der Sluys, W. G. *Inorg. Chem.* **1987**, *26*, 3182. (b) Sharp, P. R.; Schrock, R. R. *J. Am. Chem. Soc.* **1980**, *102*, 1430.
(7) Chiu, K. W.; Lyons, D.; Wilkinson, G. *Polyhedron*, **1983**, *2*, 803.

crystalline solids of **4** were obtained upon cooling a concentrated hexanes solution to −15 °C for 1 day. Yield: 0.44 g, 56% based on WCl_4.

IR data (cm^{-1}): 1367 (m), 1302 (m), 1282 (m), 1261 (m), 1161 (w, br), 1104 (m, br), 1023 (m, br), 953 (vs), 881 (w), 859 (w), 808 (s).

^1H NMR data (benzene-d_6, 24 °C, δ): 0.81 (t, $J = 7.0$ Hz, 6H, distal CH_3), 0.88 (m, 8H, $NCH_2(CH_2)_4CH_3$), 0.96 (t, $J = 7.0$ Hz, 6H, proximal CH_3), 1.15 (m, br, 8H, $NCH_2(CH_2)_4CH_3$), 1.45 (m, br, 8H, $NCH_2(CH_2)_4CH_3$), 1.60 (d, $J = 10.0$ Hz, 18H, PMe_3), 1.93 (m, br, 8H, $NCH_2(CH_2)_4CH_3$), 2.21 (m, 2H, distal $NCH_2(CH_2)_4CH_3$), 2.48 (m, 2H, distal $NCH_2(CH_2)_4CH_3$), 5.02 (m, 2H, proximal $NCH_2(CH_2)_4CH_3$), 6.03 (m, 2H, proximal $NCH_2(CH_2)_4CH_3$).

$^{31}P\{^1H\}$ NMR data (benzene-d_6, 19 °C, δ): −4.68 (s, $^1J_{W-P} = 308$ Hz, $^3J_{P-P} = 5.1$ Hz).

FAB/DIP MS (NBA, *m/z*): 1030 ($[M]^+$), 995 ($[M - Cl]^+$), 953 ($[M - PMe_3]^+$), 919 ($[M - Cl - PMe_3]^+$), 880 ($[M - 2PMe_3]^+$), 845 ($[M - NHex_2]^+$), 809 ($[M - Cl - NHex_2]^+$), 771 ($[M - NHex_2 - PMe_3]^+$), 734 ($[M - Cl - NHex_2 - PMe_3]^+$), 694 ($[M - NHex_2 - 2PMe_3]^+$).

(v) $W_2Cl_4(NEt_2)_2(PEt_2H)_2$ (5). Similar procedures as in part ii were followed to prepare $W_2Cl_4(NEt_2)_2(PEt_2H)_2$, employing PEt_2H (0.18 mL, more than 2 equiv) instead of PMe_3. Red crystals of **5** (0.31 g, 49% based on 0.5 g WCl_4) were obtained by keeping a concentrated toluene extract in a freezer at −15 °C for 1 week.

IR data (cm^{-1}): 2379 (w), 1441 (s), 1418 (w), 1353 (m), 1334 (w), 1304 (w), 1280 (w), 1262 (w), 1248 (w), 1187 (w), 1144 (w), 1093 (m), 1063 (m), 1041 (vs), 998 (s), 921 (w), 879 (ms), 835 (s), 796 (s), 755 (m), 727 (w), 706 (w), 638 (w), 590 (w), 543 (w).

^1H NMR data (benzene-d_6, 24 °C, δ): 0.66−0.81 (m, 6H, CH_3), 0.96 (t, $J = 7.0$ Hz, 6H, CH_3), 1.05−1.27 (m, 14H, CH_3 + 2 distal protons of PCH_2CH_3), 1.43 (m, 2H, distal PCH_2CH_3), 2.24 (m, 4H, proximal PCH_2CH_3 + distal NCH_2CH_3), 2.42 (m, 2H, distal NCH_2CH_3), 3.52 (m, 2H, proximal PCH_2CH_3), 4.35 (m, $^1J_{P-H} = 367$ Hz, 1H, P−H), 4.59 (m, 2H, proximal NCH_2CH_3), 6.05 (m, 2H, proximal NCH_2CH_3), 6.19 (m, $^1J_{P-H} = 367$ Hz, 1H, P−H).

$^{31}P\{^1H\}$ NMR data (benzene-d_6, 19 °C, δ): 16.20 (s, $^1J_{W-P} = 297$ Hz, $^3J_{P-P} = 5.3$ Hz).

FAB/DIP MS (NBA, *m/z*): 834 ($[M]^+$), 799 ($[M - Cl]^+$), 762 ($[M - Cl]^+$ or $[M - NEt_2]^+$), 744 ($[M - PEt_2H]^+$), 709 ($[M - Cl - PEt_2H]^+$), 673 ($[M - 2Cl - PEt_2H]^+$ or $[M - NEt_2 - PEt_2H]^+$), 654 ($[M - 2PEt_2H]^+$), 617 ($[M - Cl - 2PEt_2H]^+$), 580 ($[M - 2Cl - 2PEt_2H]^+$ or $[M - NEt_2 - 2PEt_2H]^+$).

(vi) $W_2Cl_4(NBu_2)_2(PEt_2H)_2$ (6). Compound **6** was prepared in a similar manner as **3** using PEt_2H (0.18 mL) rather than PMe_3 and obtained as bright red block-shaped crystals (0.40 g, 55% based on 0.5 g WCl_4) from a concentrated hexanes solution on standing at −15 °C for 15 h.

IR data (cm^{-1}): 2368 (m), 1416 (w), 1310 (w), 1292 (vw), 1262 (w), 1240 (vw), 1223 (vw), 1170 (w), 1144 (w), 1115 (m), 1105 (w), 1077 (w), 1044 (vs), 1035 (s), 1018 (m), 980 (w), 938 (w), 911 (s), 900 (m), 836 (s), 805 (w), 746 (m), 735 (w), 709 (m), 638 (w).

^1H NMR data (benzene-d_6, 24 °C, δ): 0.71−1.83 (m, 42H, all CH_3 + $NCH_2(CH_2)_2CH_3$ + 2 protons of PCH_2CH_3), 2.00 (m, 2H, CH_2), 2.34 (m, 4H, CH_2), 2.78 (m, 2H, CH_2), 3.60 (m, 2H, CH_2), 4.43 (m, $^1J_{P-H} = 366$ Hz, 1H, P−H), 4.80 (m, 2H, proximal CH_2), 6.26 (m, 3H, proximal CH_2 + P−H).

$^{31}P\{^1H\}$ NMR data (benzene-d_6, 19 °C, δ): 16.50 (s, $^1J_{W-P} = 297$ Hz, $^3J_{P-P} = 5.7$ Hz).

FAB/DIP MS (NBA, *m/z*): 946 ($[M]^+$), 911($[M - Cl]^+$), 856 ($[M - PEt_2H]^+$), 821 ($[M - Cl - PEt_2H]^+$), 766 ($[M - 2PEt_2H]^+$), 727 ($[M - NBu_2 - PEt_2H]^+$), 690 ($[M - 2NBu_2]^+$).

(vii) $W_2Cl_4(NHex_2)_2(PEt_2H)_2$ (7). The synthesis of **7** followed a similar course to that of **4**. Upon adding PEt_2H (0.18 mL) and with similar workup procedures using hexanes extraction, a first crop of red crystals of $W_2Cl_4(NHex_2)_2(PEt_2H)_2$ of good X-ray quality was obtained by cooling a concentrated hexanes solution to ca. 0 °C for 2 days. The supernatant liquid was allowed to crystallize further at −15 °C, and a second crop of red crystalline solid was obtained for an overall yield of 0.43 g, 54% based on 0.5 g WCl_4.

IR data (cm^{-1}): 2364 (m), 1418 (w), 1342 (w), 1304 (w), 1262 (m), 1232 (w), 1215 (vw), 1198 (vw), 1170 (m), 1147 (m), 1119 (m), 1083 (ms), 1046 (vs), 1037 (s), 937 (ms), 916 (w), 882 (ms), 839 (s), 801 (ms), 750 (m), 725 (w), 711 (m), 683 (vw), 659 (w), 642 (w).

^1H NMR data (benzene-d_6, 24 °C, δ): 0.73−1.81 (m, 58H, all CH_3 + $NCH_2(CH_2)_4CH_3$ + 2 protons of PCH_2CH_3), 2.07 (m, 2H, CH_2), 2.38 (m, 4H, CH_2), 2.85 (m 2H, CH_2), 3.59 (m, 2H, CH_2), 4.44 (m, $^1J_{P-H} = 367$ Hz, 1H, P−H), 4.89 (m, 2H, proximal CH_2), 6.28 (m, 3H, proximal CH_2 + P−H).

$^{31}P\{^1H\}$ NMR data (benzene-d_6, 19 °C, δ): 16.91 (s, $^1J_{W-P} = 296$ Hz, $^3J_{P-P} = 6.1$ Hz).

FAB/DIP MS (NBA, *m/z*): 1058 ($[M]^+$), 1024 ($[M - Cl]^+$), 968 ($[M - PEt_2H]^+$), 933 ($[M - Cl - PEt_2H]^+$), 875 ($[M - NHex_2]^+$), 839 ($[M - Cl - NHex_2]^+$), 785 ($[M - NHex_2 - PEt_2H]^+$), 692 ($[M - 2NHex_2]^+$ or $[M - NHex_2 - 2PEt_2H]^+$).

Physical Measurements. The IR spectra were recorded on a Perkin-Elmer 16PC FT-IR spectrophotometer as Nujol mulls between KBr plates. ^1H NMR spectral measurements were performed on a Varian XL-200 spectrometer operating at 200 MHz. ^1H chemical shifts are referenced to the residual proton impurity in the deuterated solvent. The $^{31}P\{^1H\}$ NMR data (81 MHz) were obtained at room temperature on a Varian XL-200 broad band spectrometer with the chemical shift values referenced externally and are reported relative to 85% H_3PO_4/D_2O. The FAB/DIP (DIP = direct insertion probe) mass spectra were acquired using a VG Analytical 70S high resolution, double focusing, sectored (EB) mass spectrometer. The instrument is equipped with a VG 11/250J data system that allowed computer control of the instrument, data recording and data processing. Samples for analysis were prepared by dissolving neat solid compound in *m*-nitrobenzyl alcohol (NBA) matrix on the direct insertion probe tip. The probe was then inserted into the instrument through a vacuum interlock and the sample bombarded with 8 keV xenon primary particles from an Ion Tech FAB gun operating at an emission current of 2 mA. Positive secondary ions were extracted and accelerated to 6 keV and then mass analyzed.

X-ray Crystallographic Procedures. Crystals of **1**, **2**, **3**, **6**, and **7** suitable for X-ray diffraction studies were obtained as described in the Experimental Section. The basic crystallographic procedures used have been fully described elsewhere.[8] The identification of the crystal systems, the collection of data, and the structure solutions and refinements are described below for each individual compound. All calculations were performed on a DEC 3000-800 AXP workstation. Data sets were corrected for decay where necessary and for Lorentz and polarization effects. Crystallographic parameters and basic information pertaining to data collection and structure refinement are summarized in Table 1. A listing of the selected bond distances and angles for **1** is presented in Table 2. Comparison tables of selected bond lengths and angles for the rest of the structures are shown in Table 3. Table 4 tabulates the important torsional angles about the W−W axis for **2**, **3**, **6**, and **7**. Tables of positional and isotropic parameters, anisotropic displacement parameters as well as complete tables of bond distances and angles and coordinates of hydrogen atoms are available as supporting information.

$W_2Cl_4(NEt_2)_2(NHEt_2)_2$ (1). An orange crystal with dimensions of 0.30 × 0.30 × 0.10 mm was attached to the end of a quartz fiber with grease and immediately transferred into a cold stream of nitrogen (−100 °C) on an Enraf-Nonius CAD-4S diffractometer equipped with graphite-monochromated Mo Kα radiation. Cell parameters consistent with that of a body-centered orthorhombic lattice were obtained by least-squares refinement of 25 well-centered reflections in the range $34 < 2\theta < 42°$. The cell dimensions and symmetry were confirmed by axial photography. A total of 1753 data were collected in the range $4 < 2\theta < 54°$ using an ω scan technique. An empirical absorption correction based on azimuthal scans of 9 reflections with Eulerian angle χ near 90° was applied to the data.[9] Examination of the systematic absences narrowed the choice of spaces groups to *Ibam* and *Iba*2. Refinement in *Ibam* space group was unsuccessful with unusually large displacement parameters for the ligand atoms, and *Iba*2 was then selected. This choice was confirmed by successful least-squares refinement. The atomic position of the metal atom W(1) was determined by direct methods as programmed in SHELXTL.[10] The remaining non-hydrogen atoms were located from subsequent least-squares refinement cycles

(8) Cotton, F. A.; Dikarev, E. V.; Wong, W. Y. *Inorg. Chem.* **1997**, *36*, 80.
(9) North, A. C. T.; Phillips, D. C.; Mathews, F. S. *Acta Crystallogr., Sect. A* **1968**, *A24*, 351.
(10) SHELXTL V. 5, Siemens Industrial Automation, Inc., 1994.

Table 1. Crystallographic Data for $W_2Cl_4(NEt_2)_2(NHEt_2)_2$ (**1**), $W_2Cl_4(NEt_2)_2(PMe_3)_2$ (**2**), $W_2Cl_4(NBu_2)_2(PMe_3)_2$ (**3**), $W_2Cl_4(NBu_2)_2(PEt_2H)_2$ (**6**), and $W_2Cl_4(NHex_2)_2(PEt_2H)_2$ (**7**)

	1	**2**	**3**	**6**	**7**
formula	$W_2Cl_4C_{16}H_{42}N_4$	$W_2Cl_4P_2C_{14}H_{38}N_2$	$W_2Cl_4P_2C_{22}H_{54}N_2$	$W_2Cl_4P_2C_{24}H_{58}N_2$	$W_2Cl_4P_2C_{32}H_{74}N_2$
fw	800.04	805.90	918.11	946.16	1058.37
space group	*Iba*2 (No. 45)	$P\bar{1}$ (No. 2)	$P\bar{1}$ (No. 2)	$P2_1/n$ (No. 14)	$P2_1/c$ (No. 14)
a, Å	11.6704(9)	9.568(2)	12.162(6)	17.970(3)	15.3937(7)
b, Å	13.336(1)	17.294(7)	14.955(4)	10.993(2)	11.473(2)
c, Å	17.321(2)	17.418(5)	18.82(1)	20.689(4)	24.977(3)
α, deg	90.0	111.82(3)	95.66(3)	90.0	90.0
β, deg	90.0	103.11(2)	97.99(4)	115.43(1)	92.33(1)
γ, deg	90.0	90.72(3)	91.26(3)	90.0	90.0
V, Å^3	2695.8(4)	2591(1)	3371(3)	3691(1)	4408(1)
Z	4	4	4	4	4
ρ_{calc}, g/cm^3	1.971	2.066	1.809	1.703	1.595
μ, mm^{-1}	8.933	9.411	7.244	14.940	5.553
radiation (λ, Å)	Mo Kα (0.710 73)	Mo Kα (0.710 73)	Mo Kα (0.710 73)	Cu Kα (1.541 84)	Mo Kα (0.710 73)
temp, °C	−100	20	−150	20	−60
R1,[a] wR2[b] [$I > 2\sigma(I)$]	0.022, 0.054	0.045, 0.119	0.058, 0.147	0.041, 0.095	0.043, 0.100
R1,[a] wR2[b] (all data)	0.028, 0.056	0.097, 0.154	0.083, 0.171	0.074, 0.113	0.055, 0.105

[a] $R1 = \Sigma||F_o| - |F_c||/\Sigma|F_o|$. [b] $wR2 = [E[w(F_o^2 - F_c^2)^2]/\Sigma[w(F_o^2)^2]]^{1/2}$.

Table 2. Selected Bond Distances (Å) and Angles (deg) and Torsion Angles (deg) for $W_2Cl_4(NEt_2)_2(NHEt_2)_2$ (**1**)

W(1)−W(1A)	2.3084(5)	W(1)−N(1)	2.198(7)
W(1)−N(2)	1.908(7)	W(1)−Cl(1)	2.384(2)
W(1)−Cl(2)	2.473(2)	W(2)−W(2A)	2.31(2)
N(1)−W(1)−N(2)	93.6(3)	N(1)−W(1)−Cl(1)	149.0(2)
N(1)−W(1)−Cl(2)	79.7(2)	N(2)−W(1)−Cl(1)	92.9(2)
N(2)−W(1)−Cl(2)	158.5(2)	Cl(1)−W(1)−Cl(2)	83.22(7)
W(1A)−W(1)−N(1)	99.6(2)	W(1A)−W(1)−N(2)	104.2(2)
W(1A)−W(1)−Cl(1)	108.02(5)	W(1A)−W(1)−Cl(2)	97.05(5)
N(1)−W(1)−W(1A)−N(1A)	107.6(4)	N(1)−W(1)−W(1A)−N(2A)	−156.1(3)
N(1)−W(1)−W(1A)−Cl(1A)	−58.2(2)	N(1)−W(1)−W(1A)−Cl(2A)	27.0(2)
N(2)−W(1)−W(1A)−N(2A)	−59.9(5)	N(2)−W(1)−W(1A)−Cl(1A)	38.1(3)
N(2)−W(1)−W(1A)−Cl(2A)	123.2(2)	Cl(1)−W(1)−W(1A)−Cl(1A)	136.0(1)
Cl(1)−W(1)−W(1A)−Cl(2A)	−138.86(8)	Cl(2)−W(1)−W(1A)−Cl(2A)	−53.7(1)

followed by difference Fourier syntheses using the SHELXL-93 structure refinement program.[11] After anisotropic refinement, a second pair of W atoms (W(2) and W(2A)), i.e. the second orientation of the W−W unit, was located. These atoms were included in the refinement, and their site occupancy factor (sof's) was allowed to vary against that of W(1) and W(1A) but was constrained so that the sum of W atoms in the molecule equaled 2. The sof's converged to final values of 0.984 for W(1) and W(1A) and 0.016 for W(2) and W(2A). Hydrogen atoms were included in the F_c calculations, but they were not refined except for the nitrogen bonded hydrogen atom H(1). Full refinement of 130 parameters resulted in the final residuals, $R = 0.022$ (for 1600 reflections with $I > 2\sigma(I)$) and $R = 0.028$ (for all 1722 data). The final difference Fourier map revealed only one peak above 1 e/Å^3, lying close to the W atoms. The absolute structure of **1** was determined to be the correct one based on the method described by Flack (Flack *x* parameter is 0.007(15)).[12]

$W_2Cl_4(NEt_2)_2(PMe_3)_2$ (2). A red crystal with dimensions of 0.30 × 0.25 × 0.10 mm was mounted and sealed inside a Lindemann capillary. Twenty-five reflections in the range $12 < 2\theta < 17°$ were centered to refine the reduced parameters corresponding to the triclinic crystal system. The diffraction data were collected at 20 °C on a Rigaku AFC7R rotating anode diffractometer using graphite-monochromated Mo Kα radiation and the ω-2θ scan technique was used to scan data points over one hemisphere of reciprocal space in the range $4 < 2\theta < 48°$ to give a total of 8125 reflections. During the whole period of data collection, three standard reflections indicated that 9.2% of intensity was lost. Empirical absorption corrections based on ψ scans of six reflections were applied to the data using the TEXSAN software package.[13] A solution was initially sought in the space group $P\bar{1}$. A three-dimensional Patterson synthesis from the SHELXS-86 package[14] provided the positions of the two W−W dinuclear units, and refinement was successful. The remaining non-hydrogen atoms were found in a series of alternating difference Fourier maps and least-squares refinements. All non-hydrogen atoms were refined anisotropically to convergence. Hydrogen atoms were placed in idealized positions. Final least-squares refinement of 439 parameters resulted in $R = 0.045$ (for 4770 reflections with $I > 2\sigma(I)$) and $R = 0.097$ (for all 8125 data). The final difference map was essentially featureless, the largest peaks being associated with the W atoms.

$W_2Cl_4(NBu_2)_2(PMe_3)_2$ (3). A rhomboidal red crystal of approximate size 0.45 × 0.24 × 0.10 mm was selected and mounted on the gonimeter head of a CAD-4S diffractometer. Indexing based on 25 reflections resulted in a triclinic cell and the cell parameters were further refined in the range $22 < 2\theta < 29°$. The intensity data were gathered by the ω-2θ scan method in the range $4 < 2\theta < 46°$. Periodically monitored check reflections showed no crystal decay during the entire period of data collection. An empirical absorption corrections based on azimuthal scans of six reflections was applied to the data set. Choice of the centrosymmetric space group $P\bar{1}$ revealed the correct positions of the W atoms via the direct-methods *E* maps using the structure solution program in SHELXS-86, and successful refinement of the structure confirmed the choice. The rest of the structure was developed by alternating difference Fourier maps and least-squares cycles. After the heavy atoms had been refined anisotropically, it became apparent that two of the four butyl chains and the carbon atoms of one PMe_3 group were disordered. This disorder was modeled by constraining the displacement parameters to be equal and restraining the chemically equivalent bonds to be approximately equal. Also, the sof's were allowed to vary but were constrained so that the sum equaled to 1. The resulting model yielded reasonable bond distances and angles. The same strategy was employed for modeling the disordered atoms of compounds **6** and **7** (*vide infra*). Hydrogen atoms were placed in

(11) Sheldrick, G. M. In *Crystallographic Computing 6*; Flack, H. D., Parkanyi, L., Simon, K., Eds.; Oxford University Press: Oxford, England, 1993; p 111.
(12) Flack, H. D. *Acta Crystallogr., Sect. A* **1983**, *A37*, 22.
(13) TEXSAN: Crystal Structure Analysis Package, Molecular Structure Corporation, Houston, TX, 1985 and 1992.
(14) Sheldrick, G. M. In *Crystallographic Computing 3*; Sheldrick, G. M., Kruger, C., Goddard, R., Eds.; Oxford University Press: Oxford, England, 1985; p 175.

Table 3. Selected Bond Distances (Å) and Angles (deg) for $W_2Cl_4(NEt_2)_2(PMe_3)_2$ (**2**), $W_2Cl_4(NBu_2)_2(PMe_3)_2$ (**3**), $W_2Cl_4(NBu_2)_2(PEt_2H)_2$ (**6**), and $W_2Cl_4(NHex_2)_2(PEt_2H)_2$ (**7**)

	2[a]	**3**[a]	**6**	**7**
W(1)−W(2)	2.329(1)	2.320(1)	2.3212(6)	2.3181(4)
W(1)−P(1)	2.530(5)	2.529(4)	2.499(3)	2.496(2)
W(2)−P(2)	2.531(4)	2.524(4)	2.507(3)	2.506(2)
W(1)−N(1)	1.93(1)	1.91(1)	1.906(8)	1.932(5)
W(2)−N(2)	1.93(1)	1.95(1)	1.908(8)	1.921(5)
W(1)−Cl(1)	2.398(4)	2.397(4)	2.394(3)	2.392(2)
W(2)−Cl(4)	2.385(4)	2.393(4)	2.387(3)	2.394(2)
W(1)−Cl(2)	2.424(4)	2.426(4)	2.424(3)	2.431(2)
W(2)−Cl(3)	2.430(4)	2.421(4)	2.431(3)	2.420(2)
P(1)−W(1)−N(1)	88.4(4)	89.7(3)	87.6(2)	86.8(2)
P(1)−W(1)−Cl(1)	153.2(2)	150.7(1)	155.6(1)	156.02(6)
P(1)−W(1)−Cl(2)	77.8(2)	76.3(1)	76.4(1)	76.58(6)
N(1)−W(1)−Cl(1)	95.0(4)	95.7(4)	98.2(2)	98.3(2)
N(1)−W(1)−Cl(2)	144.0(4)	147.2(4)	143.7(2)	145.6(2)
Cl(1)−W(1)−Cl(2)	84.3(2)	84.0(1)	85.2(1)	86.50(7)
W(2)−W(1)−P(1)	96.8(1)	98.3(1)	93.29(7)	93.28(4)
W(2)−W(1)−N(1)	105.0(4)	102.7(4)	102.3(2)	102.4(2)
W(2)−W(1)−Cl(1)	107.9(1)	108.6(1)	108.44(7)	108.28(4)
W(2)−W(1)−Cl(2)	109.5(1)	108.5(1)	110.85(8)	108.41(5)
P(2)−W(2)−N(2)	88.7(3)	88.9(4)	88.3(3)	86.1(2)
P(2)−W(2)−Cl(3)	76.6(1)	76.6(2)	76.6(1)	77.49(7)
P(2)−W(2)−Cl(4)	152.2(2)	152.7(1)	156.61(9)	156.69(6)
N(2)−W(2)−Cl(3)	145.2(4)	146.1(4)	143.1(2)	143.9(2)
N(2)−W(2)−Cl(4)	95.8(3)	96.3(4)	98.0(3)	97.9(2)
Cl(3)−W(2)−Cl(4)	84.4(2)	84.6(2)	85.2(1)	86.17(7)
W(1)−W(2)−P(2)	98.1(1)	97.2(1)	93.47(6)	94.02(5)
W(1)−W(2)−N(2)	103.9(4)	103.9(4)	102.1(2)	102.8(2)
W(1)−W(2)−Cl(3)	109.4(1)	108.2(1)	112.15(7)	110.12(5)
W(1)−W(2)−Cl(4)	107.4(1)	107.6(1)	107.03(7)	107.28(5)

[a] Distances and angles are the averages for the two independent molecules of the asymmetric unit

Table 4. Selected Torsion Angles (deg) about the W−W Axis for $W_2Cl_4(NEt_2)_2(PMe_3)_2$ (**2**), $W_2Cl_4(NBu_2)_2(PMe_3)_2$ (**3**), $W_2Cl_4(NBu_2)_2(PEt_2H)_2$ (**6**), and $W_2Cl_4(NHex_2)_2(PEt_2H)_2$ (**7**)

	2[a]	**3**[a]	**6**	**7**
P(1)−W(1)−W(2)−Cl(3)	45.0(2)	45.5(2)	57.2(1)	59.89(7)
P(1)−W(1)−W(2)−Cl(4)	−45.1(2)	−44.6(1)	−34.5(1)	−32.38(6)
N(1)−W(2)−W(2)−N(2)	−55.8(5)	−54.4(5)	−48.6(3)	−47.6(2)
N(1)−W(1)−W(2)−Cl(4)	45.1(4)	47.0(3)	53.8(3)	55.1(2)
Cl(1)−W(1)−W(2)−P(2)	−46.0(2)	−44.4(2)	−34.5(1)	−31.34(7)
Cl(1)−W(1)−W(2)−N(2)	44.7(4)	46.2(4)	54.5(3)	55.6(2)
Cl(2)−W(1)−W(2)−P(2)	44.2(2)	45.4(2)	57.3(1)	61.08(7)
Cl(2)−W(1)−W(2)−Cl(3)	−34.4(2)	−32.7(2)	−19.6(1)	−17.06(8)

[a] Torsion angles are the averages for the two independent molecules of the asymmetric unit.

idealized positions but they were not refined. Full refinement of 570 parameters led to residuals of $R = 0.058$ (for 7435 reflections with $I > 2\sigma(I)$) and $R = 0.083$ (for all 9356 data). The final difference Fourier map showed no significant peaks other than those located in the vicinity of the W atoms.

$W_2Cl_4(NBu_2)_2(PEt_2H)_2$ (6). A red crystal with dimensions of 0.25 × 0.18 × 0.15 mm was glued on the tip of a glass fiber with epoxy cement. Diffraction data were collected at 20 °C on a Rigaku AFC5R diffractometer using Cu Kα radiation. A least-squares analysis of the setting angles of 25 reflections with $18 < 2\theta < 37°$ provided accurate unit cell parameters (Table 1). Three standard reflections were measured during data collection, and displayed 9.5% decay in intensity. A total of 5496 reflections in the range $5 < 2\theta < 120°$ were collected using the ω-2θ scan technique. Empirical absorption corrections based on ψ scans of 6 reflections were applied to the data using the TEXSAN software package.[13] The space group was assigned as $P2_1/n$ from the systematic absences in the data. It was found that two of the four butyl chains and the ethyl groups of both PEt_2H ligands were disordered. Hydrogen atoms were placed in idealized positions and were not refined except for those bonded to P atoms. Final least-squares refinement of 301 parameters resulted in $R = 0.041$ (for 4002 reflections with $I > 2\sigma(I)$) and $R = 0.074$ (for all 5491 data). The largest remaining peak in the final difference Fourier map was 0.74 e/Å^3.

$W_2Cl_4(NHex_2)_2(PEt_2H)_2$ (7). A red crystal with dimensions of 0.45 × 0.25 × 0.08 mm was mounted on the tip of a quartz fiber with grease and quickly placed in the cold stream at −60 °C of an Enraf-Nonius low-temperature controller, Model FR 558-S. Intensity data were collected on an Enraf-Nonius FAST diffractometer with an area detector for $4 < 2\theta < 51°$ using Mo Kα radiation. The general procedures have been fully described elsewhere.[15] A preliminary data collection was first carried out to afford all parameters and an orientation matrix. Fifty reflections were used in cell indexing and 250 reflections in cell refinement. Axial images were used to confirm the Laue group and cell dimensions. The data were corrected for Lorentz and polarization effects by the MADNES program.[16] Systematic absences of the data uniquely determined the space group to be $P2_1/c$. The coordinates of the metal atoms were provided by direct methods in SHELXTL and the structure refinement was conducted with the SHELXL-93 software package employing all data and full matrix least-squares refinement on F^2. The data were corrected for absorption anisotropy effects using a local adaptation of the program SORTAV.[17] After anisotropic refinement of the heavy atoms, it became apparent that all four hexyl chains and one of the CH_3 groups in the PEt_2H ligand were disordered. All hydrogen atoms were included in the structure factor calculations at idealized positions and were allowed to ride on the neighboring carbon atoms except for those bonded to P atoms, which were refined. Final least-squares refinement of 371 parameters resulted in residuals $R = 0.043$ (for 6672 reflections with $I > 2\sigma(I)$) and $R = 0.055$ (for all 7833 data). The largest peak in the final difference Fourier map was 2.31 e/Å^3, lying 1.26 Å from W(1).

Results and Discussion

Synthesis. Treatment of $W_2Cl_6(THF)_4$ with diethylamine (≥2 equiv) in tetrahydrofuran produces the triply-bonded ditungsten species $W_2Cl_4(NEt_2)_2(NHEt_2)_2$ (**1**) as orange crystals in ca. 70% yield. The preparative procedure used incorporates the methodology developed by Bradley and co-workers to prepare the analogous *tert*-butylamido complex $W_2Cl_4(NHCMe_3)_2(NH_2CMe_3)_2$ (eq 1).[3a] However, complex **1** was found to adopt a cis stereochemistry, in contrast to the trans one observed in $W_2Cl_4(NHCMe_3)_2(NH_2CMe_3)_2$. Upon addition of an excess of PMe_3 (>2 equiv) to a THF solution of **1**, the coordinated amine ligands in **1** are replaced by the monodentate phosphines to afford a new W_2^{6+} complex $W_2Cl_4(NEt_2)_2(PMe_3)_2$ (**2**) in good yield. Unlike $W_2Cl_4(NHCMe_3)_2(PR_3)_2$ molecules, compound **2** adopts a staggered geometry due to the absence of intramolecular hydrogen bonding.[3b,18a] Scheme 1 shows the reaction pathways leading to $W_2Cl_4(NR_2)_2(PR'_3)_2$ molecules starting from $W_2Cl_6(THF)_4$. In fact, this synthetic route has proved to be general and can be employed to prepare other $W_2Cl_4(NR_2)_2(PR'_3)_2$ molecules with amido groups of varying sizes. Another five new ditungsten complexes, viz. $W_2Cl_4(NR_2)_2(PMe_3)_2$ (R = Bu (**3**), Hex (**4**)) and $W_2Cl_4(NR_2)_2(PEt_2H)_2$ (R = Et (**5**), Bu (**6**), Hex (**7**)) have been isolated in similar yields, and we believe that $W_2Cl_4(NR_2)_2(NHR_2)_2$ (R = Bu, Hex) are the probable intermediate species in each case. It is also clear that the stereochemistry of the products is preserved upon substitution by the phosphine ligands. So, there is no rearrangement of ligands in this reaction. On the contrary, it has been reported that both the *trans* and *cis* isomers of $W_2Cl_4(NHCMe_3)_2(PR_3)_2$ were obtained when the intermediate complex *trans*-$W_2Cl_4(NHCMe_3)_2(NH_2CMe_3)_2$ was allowed to react with monodentate phosphines.[3b,18a]

(15) Bryan, J. C.; Cotton, F. A.; Daniels, L. M.; Haefner, S. C.; Sattelberger, A. P. *Inorg. Chem.* **1995**, *34*, 1875.
(16) Pflugrath, J.; Messerschmitt, A. MADNES, Munich Area Detector (New EEC) System, version EEC 11/9/89, with enhancements by Enraf-Nonius Corp., Delft, The Netherlands. A description of MADNES appears in: Messerschmitt, A.; Pflugrath, J. *J. Appl. Crystallogr.* **1987**, *20*, 306.
(17) Blessing, R. H. *Acta Crystallogr., Sect. A* **1995**, *A51*, 33.
(18) (a) Cotton, F. A.; Yao, Z. *J. Cluster Sci.* **1994**, *5*, 11. (b) Chen, H.; Cotton, F. A.; Yao, Z. *Inorg. Chem.* **1994**, *33*, 4255.

Scheme 1

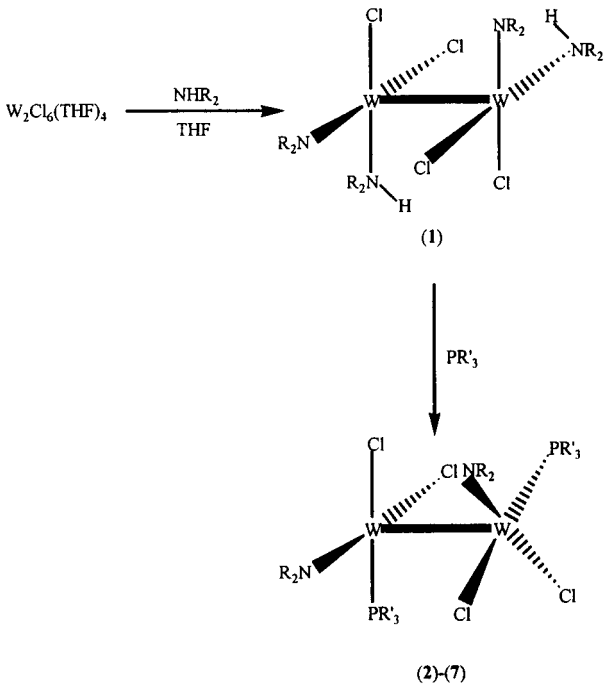

Each of the compounds **1**−**7** is soluble in toluene and benzene but only complexes **3**, **4**, **6**, and **7** dissolve well in hexanes, presumably due to the presence of the hydrophobic alkyl tails in these complexes. Solutions of compounds of this type are prone to air oxidation and slowly decompose upon exposure. Evidence for this was found in the $^{31}P\{^1H\}$ NMR spectra of **2**−**4**, which showed significant amounts of $WOCl_2(PMe_3)_3$,[7] especially when the spectrum was recorded at a high temperature. Upon heating, no evidence of cis−trans isomerization was observed for $W_2Cl_4(NR_2)_2(PR'_3)_2$ molecules but a small amount of the quadruply-bonded compound $W_2Cl_4(PMe_3)_4$ formed in these cases. Its origin is still not yet clear, though some speculations have been put forward before for $W_2Cl_4(NHCMe_3)_2(PR_3)_2$ (R = Me, Et, Pr^n).[18b]

On the other hand, we observed that similar compounds were not isolated for the more bulky phosphine PPh_3 and the dicyclohexylamido groups.

Spectroscopy. The infrared spectrum of $W_2Cl_4(NEt_2)_2(NHEt_2)_2$ exhibits characteristic ν(N−H) stretching vibrations at 3182 cm^{-1} corresponding to the coordinated diethylamine ligands. The presence of PEt_2H ligands in **5**−**7** is discernible from the IR spectral peaks within the short range 2364−2379 cm^{-1} due to ν(P−H). All the complexes reported herein show mass spectral peaks assignable to parent ions, M^+, as well as fragment ions produced by sequential loss of amido, chlorine and amine (for **1**) or phosphine (for **2**−**7**) ligands. Loss of chlorine ligands during fragmentation is competitive with loss of amido, amine, and phosphine ligands. For **1**, the most intense peak occurs at *m/z* 654 and the most abundant fragment ion for the rest of the compounds is $[W_2Cl_3(NR_2)_2(PR'_3)]^+$ in each case. Rupture of the metal−metal bond is not a major fragmentation pattern for these complexes under the experimental conditions.

In the ^1H NMR spectrum of **1** in $CDCl_3$, a broad signal which integrates as two protons is observed at δ 5.26 attributable to $NHEt_2$ groups. The ^1H NMR spectra of **2**−**7** all show that the diethylamine ligands have been completely replaced by phosphine ligands. At room temperature, each of the compounds **2**−**4** clearly displays two distinguishable triplets due to the methyl groups and two separate pairs of multiplets due to the methylene groups. Such a marked difference in chemical shifts between the methyl groups as well as the methylene groups has been discussed previously for $M_2(NMe_2)_6$ (M = Mo or W)[19] and $W_2Cl_2(NEt_2)_4$,[1b] where considerable magnetic anisotropic effects imparted by a metal−metal triple bond is one of the explanations. On the basis of this assignment, the downfield and upfield resonances are assigned to the proximal and distal groups respectively in our compounds. As in $M_2Cl_4(NMe_2)_2L_2$ (M = Mo or W; L = PMe_3 or PMe_2Ph) molecules,[4] the well-separated proximal and distal NEt resonances are consistent with frozen out rotations about the W−N bonds at room temperature, and there is also no indication for proximal−distal exchange from the high-temperature spectra. On the other hand, no attempt has been made to fully assign the ^1H NMR spectra of **5**−**7**; because of the complexity. All the NEt_2 protons are partially obscured by the resonances due to the PEt_2H groups.

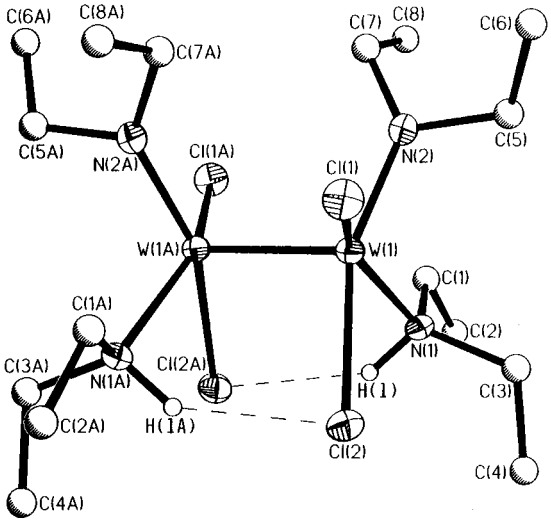

Figure 1. Perspective drawing of $W_2Cl_4(NEt_2)_2(NHEt_2)_2$ (**1**). Atoms are represented by thermal ellipsoids at the 40% probability level. Carbon atoms are shown as spheres of arbitrary radii. Two hydrogen bonds N−H···Cl are shown as dashed lines.

The $^{31}P\{^1H\}$ NMR spectra of all $W_2Cl_4(NR_2)_2(PR'_3)_2$ molecules exhibit strong central singlets flanked by satellites peaks due to coupling to the ^{183}W nuclei. The data are shown in the Experimental Section. As in the case of $W_2Cl_4(NHCMe_3)_2(PR_3)_2$ molecules, the satellites can usually serve as a probe for identifying different isomers of the reaction products.[18b] Here, the magnitude of the one-bond P−W coupling constant of about 300 Hz and the appearance of the satellites as doublets in each case are useful indicators of the formation of a *cis* isomer. The splitting observed in the satellites is proportional to $^3J_{P-P}$ and the $^3J_{P-P}$ values lie in the range 5−6 Hz. It is obvious that the $^{31}P\{^1H\}$ NMR chemical shifts and the corresponding coupling constants in each case are relatively insensitive to the change of amido ligands.

Molecular Structures. Compound **1** conforms to the noncentrosymmetric space group *Iba*2 with four molecules per unit cell. The structure of one molecule is depicted in Figure 1, and the important molecular dimensions are presented in Table 2. It consists of two $WCl_2(NEt_2)(NHEt_2)$ fragments bound by a W−W triple bond with the amine and amide groups cis to each other in each fragment. There is a 1.6% orientational disorder of the W−W vector in the molecule (Figure 2). The W−W distance (2.3084(5) Å) is somewhat longer than in $W_2Cl_4(NHCMe_3)_2(NH_2CMe_3)_2$ (2.288(3) Å).[3a] No disorder of the N atoms was observed and the distinction between the amide and amine groups can be easily revealed from the difference in

(19) (a) Chisholm, M. H.; Cotton, F. A.; Frenz, B. A.; Reichert, W. W.; Shive, L. W.; Stults, B. R. *J. Am. Chem. Soc.* **1976**, *98*, 4469. (b) Chisholm, M. H.; Cotton, F. A.; Extine, M.; Stults, B. R. *J. Am. Chem. Soc.* **1976**, *98*, 4477.

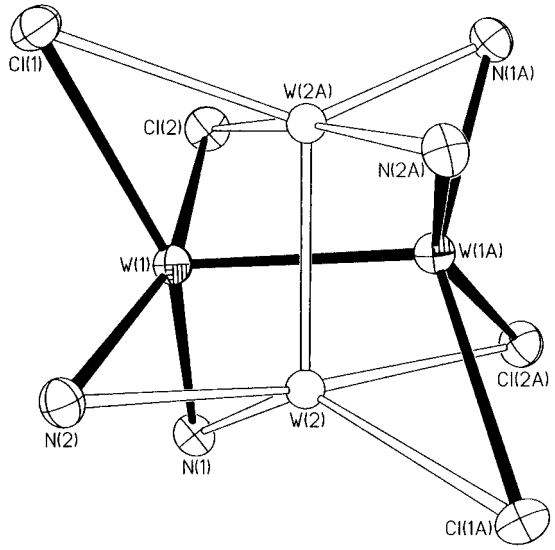

Figure 2. Drawing showing the two orientations of the W_2 unit in $W_2Cl_4(NEt_2)_2(NHEt_2)_2$. Carbon atoms are omitted for clarity.

W−N distances. The bond distances W(1)−N(1) and W(1)−N(2) are respectively 2.198(7) and 1.908(7) Å which match well with those previously reported for W−$NHMe_2$ (2.28 Å)[2a] and W−NEt_2 (1.936 Å)[1b]. Apart from the different W−N distances, we were able to locate the hydrogen atom bonded to N(1) from the Fourier map and refinement was successful. It is also noteworthy that the angles N(1)−W(1)−Cl(2) (79.7°) and N(2)−W(1)−Cl(1) (92.9°) are significantly different, presumably because of the intramolecular hydrogen-bonding interaction between the hydrogen atom on N(1) and Cl(2) on the same W atom (N(1)−H···Cl(2), 2.85 Å). The W−Cl distance is ca. 0.09 Å longer for the bond trans to the NEt_2 ligand relative to that trans to the $NHEt_2$ ligand. While a strong N−H···Cl intramolecular hydrogen bonding is retained in this complex, each molecule deviates from an ideal eclipsed geometry with the torsion angle involving the hydrogen bonded N(1) and Cl(2A) atoms across the W−W vector being 27.0° (Figure 3a). The N−H···Cl distance is 2.303 Å.

Compounds **2** and **3** both crystallize in the triclinic space group $P\bar{1}$ whereas compounds **6** and **7** in the monoclinic space group $P2_1/n$ and $P2_1/c$ respectively. For **2** and **3**, there are two independent molecules per asymmetric unit. Perspective views of the molecular structures of **2**, **3**, **6**, and **7** are shown in Figures 4−7, respectively. The important bond parameters of these four $W_2Cl_4(NR_2)_2(PR'_3)_2$ molecules are collected and compared in Table 3. Each of the structures possesses a common W_2^{6+} unit having eight separate unidentate ligands and the internal parameters for the $W_2Cl_4N_2P_2$ cores of them are not surprisingly very similar. The two pseudoplanar $WCl_2(NR_2)(PR'_3)$ fragments united by a W≡W bond are staggered with respect to each other (Figure 3b). The staggered configuration is to be expected because the W−W triple bond imposes no rotational barrier, and it is basically the nonbonded repulsions between ligated atoms that account for the observed rotational conformation. This also reflects the important role of hydrogen bonding in enforcing an essentially eclipsed configuration for $W_2Cl_4(NHCMe_3)_2(PR_3)_2$ molecules even when no δ bond exists. Each W atom is four-coordinate and the phosphine and amido ligands are arranged in a cis configuration. This is in accord with the stereochemistry of the intermediate **1** formed in the initial step with a cis configuration. The W−W distances span the narrow range of 2.318−2.329 Å and are characteristic of a triple bond between W atoms. Comparison with other triply-bonded tungsten complexes indicates that the W−W bond distances of **2**, **3**, **6**, and **7** are comparable to those observed for $W_2Cl_3(NMe_2)_3(PMe_2Ph)_2$ (2.338(1) Å) and $W_2Cl_4(NMe_2)_2(PMe_2Ph)_2$ (2.322(1) Å)[4] but slightly longer than those in $W_2Cl_2(NMe_2)_4$ (2.285(2) Å)[1a] and $W_2Cl_2(NEt_2)_4$ (2.301(1) Å).[1b] Such a lengthening is probably a consequence of the steric interactions across the W_2^{6+} center. The W−N bond lengths in each of the complexes **2**, **3**, **6** and **7** (Table 3) are normal distances for a tungsten alkylamide bond and are comparable to those for $W_2Cl_3(NMe_2)_3(PMe_2Ph)_2$ and $W_2Cl_4(NMe_2)_2(PMe_2Ph)_2$ (ca. 1.93 Å), corresponding to a formal W−N double bond. In each case, it is also evident that the mean W−Cl distances, trans to N, are longer than those trans to P. These seem to be manifestations of the stronger trans influence of NR_2 groups than the phosphine ligands toward the chlorine atoms in these complexes. Also, it was our intention to switch the monophosphine from PMe_3 to another one bearing a hydrogen atom on it, namely PEt_2H, so as to see any possibility of hydrogen bonding interaction in this case and hence further investigate the effect of such a bond in this class of compounds. As expected, the hydrogen atoms bonded to the P atoms are capable of forming hydrogen bonds with the Cl atoms on the adjacent W atom (average P−H···Cl distance, 2.91 Å for **6**; 2.97 Å for **7**). This causes a significant decrease in the torsion angles P(1)−W(1)−W(2)−Cl(4) and Cl(1)−W(1)−W(2)−P(2) for **6** and **7** by more than 10° from the perfect staggered geometry

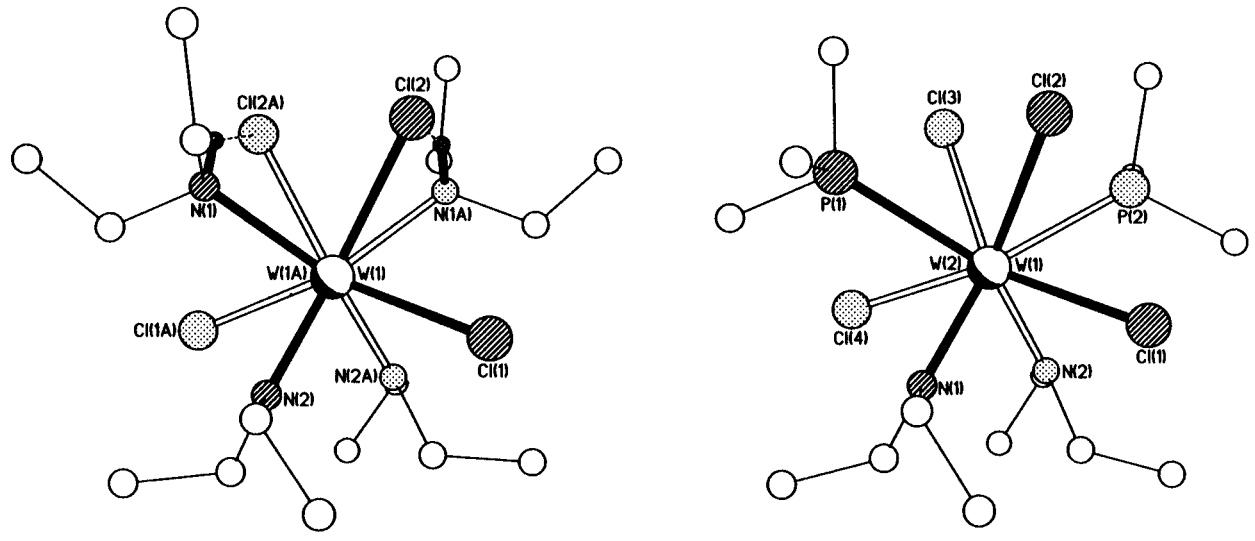

Figure 3. Views of the central part of molecules **1** (**a**) and **2** (**b**) directly down the W−W axis. Only tungsten and their neighboring atoms are labeled for clarity.

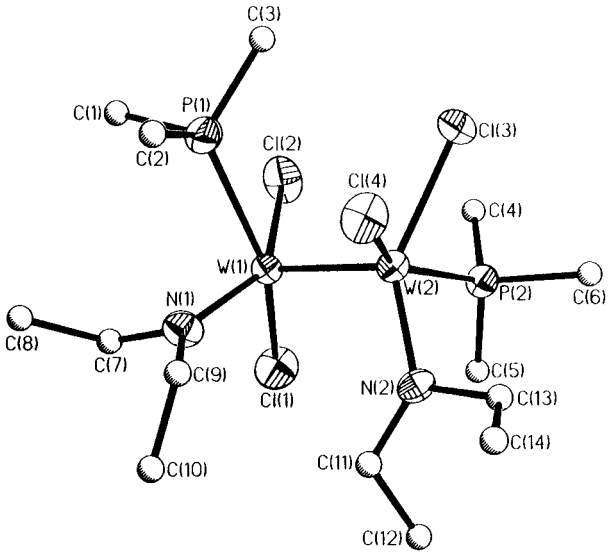

Figure 4. Perspective drawing of $W_2Cl_4(NEt_2)_2(PMe_3)_2$ (**2**). Atoms are represented by thermal ellipsoids at the 40% probability level. Carbon atoms are shown as spheres of arbitrary radii.

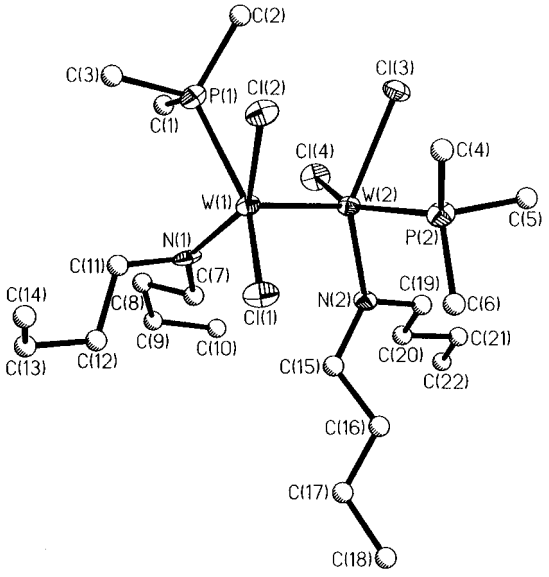

Figure 5. Perspective drawing of $W_2Cl_4(NBu_2)_2(PMe_3)_2$ (**3**). Only the major orientation of the carbon atoms is shown. Atoms are represented by thermal ellipsoids at the 40% probability level. Carbon atoms are shown as spheres of arbitrary radii.

(Table 4). Furthermore, in the structures of compounds **3**, **6**, and **7**, severe disordering problem was encountered for the carbon atoms associated with the dibutyl and dihexyl groups as well as PEt_2H ligands.

Concluding Remarks

A two-step synthesis leading to $W_2Cl_4(NR_2)_2(PR'_3)_2$-type molecules from the reaction of $W_2Cl_6(THF)_4$ with the dialkylamine, followed by phosphine substitution, is described. The successful isolation and characterization of a plausible intermediate species $W_2Cl_4(NEt_2)_2(NHEt_2)_2$ allows us to understand the elementary reaction pathways in these reactions. However, it must be noted that there is still uncertainty about the existence of any other isomers of $W_2Cl_4(NR_2)_2(NHR_2)_2$ in the solution mixture during the initial step, even though *in situ* $^{31}P\{^1H\}$ NMR studies upon phosphine addition revealed the title *cis* isomer of $W_2Cl_4(NR_2)_2(PR'_3)_2$ to be the only phosphine-containing ditungsten products. It is also noteworthy that in all of the

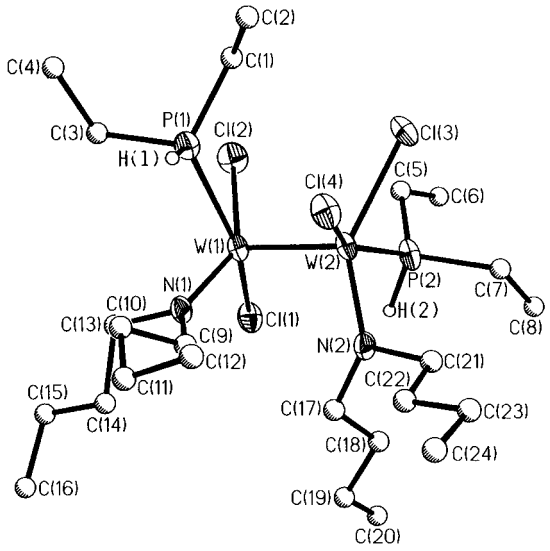

Figure 6. Perspective drawing of $W_2Cl_4(NBu_2)_2(PEt_2H)_2$ (**6**). Only the major orientation of the carbon atoms is shown. Atoms are represented by thermal ellipsoids at the 40% probability level. Carbon atoms are shown as spheres of arbitrary radii, and only hydrogen atoms on the PEt_2H ligands are shown.

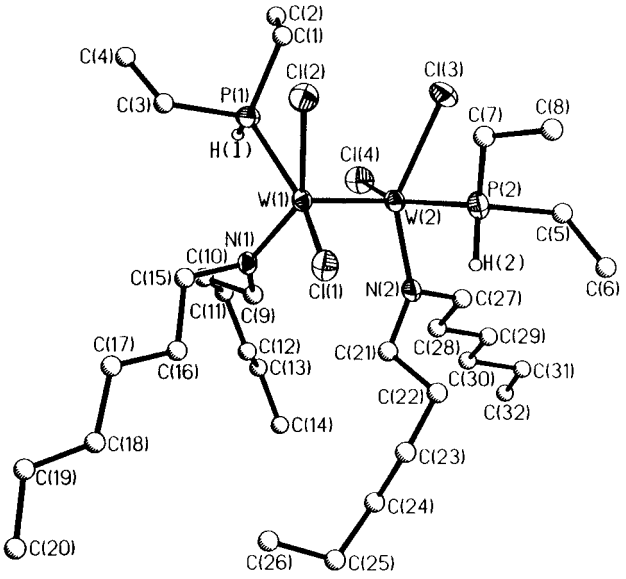

Figure 7. Perspective drawing of $W_2Cl_4(NHex_2)_2(PEt_2H)_2$ (**7**). Only the major orientation of the carbon atoms is shown. Atoms are represented by thermal ellipsoids at the 40% probability level. Carbon atoms are shown as spheres of arbitrary radii and only hydrogen atoms on the PEt_2H ligands are shown.

compounds reported here, the stereochemistry corresponds to the same type of *cis* isomer previously reported.[18] The other possible *cis* isomer still remains unobserved, and the question of why still remains unanswered.

Acknowledgment. We are grateful to the National Science Foundation for financial support. We also thank the Department of Chemistry, The University of Hong Kong, for providing the diffractometer facilities for the X-ray data collection of compound **2** during the leave of absence of W.-Y.W. in Hong Kong.

Supporting Information Available: Five X-ray crystallographic files, in CIF format, are available. Access and/or ordering information is given on any current masthead page.

IC9610694